Analysis of Gas Flow Distribution in a Fluidized Bed Using Two-Fluid Model with Kinetic Theory of Granular Flow and Coupled CFD-DEM: A Numerical Study

Matija Založnik - Matej Zadravec ☐ Faculty of Mechanical Engineering, University of Maribor, Slovenia ☐ matej.zadravec@um.si

Abstract Fluidized bed systems are widely used in chemical and process engineering due to their excellent heat and mass transfer properties. Numerical modeling plays a crucial role in understanding and optimizing these systems, with the two-fluid model enhanced by the kinetic theory of granular flow (TFM-KTGF) and the coupled computational fluid dynamics-discrete element method (CFD-DEM) emerging as leading techniques. This study employs both models to simulate gas-solid interactions and evaluates their performance using a benchmark single-spout fluidized bed case validated against experimental data. Subsequently, the influence of particle presence on gas flow distribution through a non-uniform distribution plate is analyzed. The results show that the common assumption of proportional flow distribution based on the opening area fraction is inaccurate, particularly in the presence of particles. Both numerical models capture this behavior, with TFM-KTGF showing trends comparable to the coupled CFD-DEM approach but at significantly reduced computational cost. The findings highlight the importance of accounting for particle dynamics in distribution plate design and promote the TFM-KTGF approach as a promising alternative for large-scale simulations.

Keywords fluidized bed, distribution plate, two-fluid model with kinetic theory of granular flow, coupled CFD-DEM, flow distribution

Highlights

- Two models (TFM-KTGF and CFD-DEM) simulate gas-solid flow in fluidized beds.
- Models validated against experiments, showing good particle behavior prediction.
- Gas flow depends on particles, not just plate geometry.
- CFD-DEM captures local effects; TFM-KTGF is faster and predicts overall trends.

1 INTRODUCTION

Fluidized bed systems are widely used in various industrial applications due to their excellent heat and mass transfer characteristics. Their applications range from chemical reactors and drying processes to coating technologies and catalytic cracking. Despite these advantages, fluidized beds remain inherently complex systems, where interactions between the gas and solid phases must be thoroughly understood to ensure efficient and stable operation [1,2].

With recent advances in computational modeling, the two-fluid model with added kinetic theory of granular flow (TFM-KTGF) and the coupled computational fluid dynamics-discrete element method (CFD-DEM) have emerged as powerful tools for simulating the complex behavior of fluidized bed systems. The TFM-KTGF approach treats both the gas and solid phases as interpenetrating continua within the Eulerian-Eulerian framework, with kinetic theory of granular flow (KTGF) playing a key role in characterizing particle behavior and inter-particle interactions. In contrast, the coupled CFD-DEM approach models the motion and interactions of individual particles in a Lagrangian framework, while the gas phase is treated using computational fluid dynamics (CFD) in the Eulerian framework. Although the coupled CFD-DEM approach provides a detailed resolution of particle dynamics, its complexity and high computational cost make it less practical for large-scale simulations compared to TFM-KTGF [3].

Esgandari et al. [4] conducted a direct comparison between these two modeling approaches in fluidized single- and multi-spout bed systems. Their study demonstrated that the TFM-KTGF approach could successfully replicate key hydrodynamic features observed in the more computationally intensive coupled CFD-DEM approach. Similarly, Ostermeier et al. [5] compared both numerical models for gas-solid fluidized beds and reported consistent global trends between them. These findings highlight why the TFM-KTGF approach is increasingly favored in both research and industry, offering reduced computational times while maintaining comparable predictive accuracy. Additional studies have examined the capabilities and limitations of both models through practical multiphase case studies of fluidized bed systems [6-9].

Flow distribution plays a crucial role in the proper functioning of fluidized bed systems, directly influencing particle mixing and the effectiveness of heat and mass transfer. One of the most essential components for ensuring optimal flow is the gas distribution plate (also referred to as the distributor), which governs the efficiency of gas introduction into the particle bed. Numerous designs for distribution plates have been proposed in the literature for various applications [10,11]. A numerical analysis of gas flow distribution across a distribution plate in a Wurster coater setup was performed by Kevorkijan et al. [12], using the coupled CFD-DEM approach. Their study revealed that both particle loading and inlet airflow rate significantly impact the uniformity of gas distribution across the distribution plate.

Recent studies have further examined distributor performance, pressure drop, and mixing efficiency in both industrial and laboratory systems, emphasizing that distributor geometry and particle properties critically influence hydrodynamic behavior inside the system. Gonzalez-Arango and Herrera [13] used CFD to study how

DOI: 10.5545/sv-jme.2025.1365

the geometries of different gas-phase distributors inside the fluidized bed affect the pressure drop and particle mixing. Their findings highlight that both the physical design and material selection of distribution plates can substantially impact system performance. The optimization of a uniform distributor inside a fluidized reactor was carried out by Singh et al. [14] using CFD, providing an example of the effective use of modeling tools for equipment optimization.

Although distribution plates are often designed based on open area fractions, this geometric assumption neglects particle effects that can significantly modify local gas flow through resistance, clustering, and particle-fluid interactions. While TFM-KTGF and coupled CFD-DEM have been widely used to analyze fluidized bed hydrodynamics, few studies have investigated how particles influence gas distribution through non-uniform distribution plates. To address this gap, the present study employs both TFM-KTGF and coupled CFD-DEM modeling to evaluate deviations from theoretical, area-based flow distributions and to provide insights for more accurate distribution plate design. This approach improves our understanding of why simplified assumptions sometimes fail in real-world applications, especially when complex physical phenomena are involved. The analysis was conducted on a laboratory-scale fluidized bed equipped with a distribution plate featuring non-uniform opening sizes, as shown in Fig. 1.

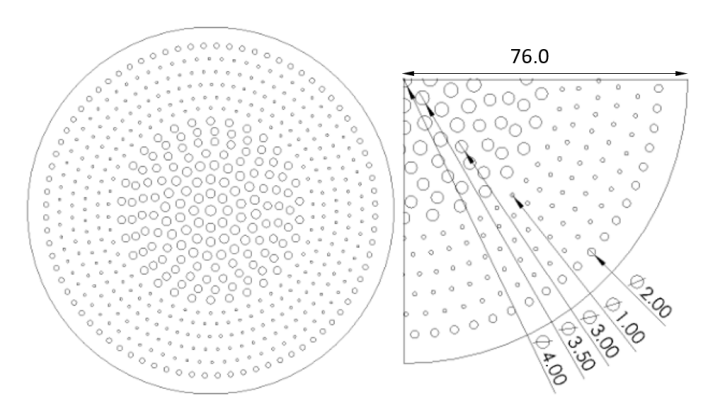


Fig. 1. A distribution plate with non-uniform opening sizes in a laboratory-scale fluidized bed system was used for the numerical analysis

2 METHODS

2.1 Two-Fluid Model with Kinetic Theory of Granular Flow

In the TFM approach, both the gas and solid phases are treated as independent continua, each governed by its own set of conservation equations. For a non-reactive, transient, isothermal system composed of spherical particles, the governing equations for mass and momentum conservation are expressed as follows:

$$\frac{\partial}{\partial t} \left(\alpha_g \rho_g \right) + \nabla \left(\alpha_g \rho_g \mathbf{v}_g \right) = 0, \tag{1}$$

$$\frac{\partial}{\partial t} (\alpha_s \rho_s) + \nabla (\alpha_s \rho_s \mathbf{v_s}) = 0, \tag{2}$$

$$\frac{\partial}{\partial t} (\alpha_{g} \rho_{g} \mathbf{v}_{g}) + \nabla (\alpha_{g} \rho_{g} \mathbf{v}_{g} \mathbf{v}_{g}) =
= -\alpha_{g} \nabla p + \nabla \tau_{g} + \alpha_{g} \rho_{g} \mathbf{g} + \beta (\mathbf{v}_{s} - \mathbf{v}_{g}),$$
(3)

$$\frac{\partial}{\partial t} (\alpha_s \rho_s \mathbf{v}_s) + \nabla (\alpha_s \rho_s \mathbf{v}_s \mathbf{v}_s) =
= -\alpha_s \nabla p - \nabla p_s + \nabla \tau_s + \alpha_s \rho_s \mathbf{g} + \beta (\mathbf{v}_g - \mathbf{v}_s),$$
(4)

where the subscripts g and s denote the gas and solid phases, respectively. Here, α_i represents the volume fraction, ρ_i the density, v_i the velocity, p_s the solid pressure, τ_i the stress tensor, g the gravitational acceleration, and β the momentum exchange coefficient, which is computed using a drag model. The solid pressure and the stress tensor of the solid phase are calculated as follows:

$$p_s = \alpha_s \rho_s \Theta_s + 2\rho_s (1 + e_{ss}) \alpha_s^2 g_{0ss} \Theta_s, \tag{5}$$

$$\boldsymbol{\tau}_{i} = \boldsymbol{\mu}_{s} \left[\nabla \mathbf{v}_{s} + \left(\nabla \mathbf{v}_{s} \right)^{T} \right] + \lambda_{s} \left(\nabla \mathbf{v}_{s} \right), \tag{6}$$

where Θ_s is the granular temperature, e_{ss} is the restitution coefficient, $g_{0,ss}$ is the radial distribution function, μ_s is the granular viscosity, and λ_s is the bulk viscosity. The radial distribution function is a correction factor that accounts for the increased probability of particle collisions as the solid phase becomes dense. It is calculated using the following equation:

$$g_{0,ss} = \left[1 - \sqrt[3]{\frac{\alpha_s}{\alpha_{s,max}}}\right]^{-1},\tag{7}$$

where $\alpha_{s,max}$ represents the packing limit. The granular viscosity, which is related to the particle motion and interactions, is calculated using the following expressions [15,16]:

$$\mu_s = \mu_{s,kin} + \mu_{s,col},\tag{8}$$

$$\mu_{s,kin} = \frac{\alpha_s d_s \rho_s \sqrt{\Theta_s \pi}}{6(3 - e_{ss})} \left[1 + \frac{2}{5} (1 + e_{ss}) (3e_{ss} - 1) \alpha_s g_{0,ss} \right], \tag{9}$$

$$\mu_{s,col} = \frac{4}{5} \alpha_s \rho_s d_s g_{0,ss} \left(1 + e_{ss} \right) \sqrt{\frac{\Theta_s}{\pi}}. \tag{10}$$

where d_s is the particle diameter. The bulk viscosity characterizes the material's response to changes in pressure and stress and is calculated by the equation proposed by Lun et al. [17]:

$$\lambda_s = \frac{4}{3} \alpha_s \rho_s d_s g_{0,ss} \left(1 + e_{ss} \right) \sqrt{\frac{\Theta_s}{\pi}}.$$
 (11)

The granular temperature Θ_s is a parameter introduced into the two-fluid model (TFM) through the KTGF. It quantifies the random fluctuations in particle velocity arising from collisions. The transport equation for the granular temperature is given as follows:

$$\frac{3}{2} \left[\frac{\partial}{\partial t} (\alpha_s \rho_s \Theta_s) + \nabla (\alpha_s \rho_s \mathbf{v}_s \Theta_s) \right] = \\
= (-p_s \mathbf{I} + \mathbf{\tau}_s) : \nabla \mathbf{v}_s + \nabla (\kappa_{\Theta} \nabla \Theta_s) - \gamma_{\Theta} + \phi_{ss}, \tag{12}$$

where **I** is the identity tensor, κ_{Θ_s} is the diffusion coefficient, γ_{Θ_s} represents the collisional dissipation of energy, and ϕ_{gs} denotes the interphase energy transfer due to particle-gas interactions. The first term on the right-hand side of the granular temperature equation corresponds to energy production; the second term represents the diffusion of granular temperature; the third accounts for energy dissipation due to particle collisions; and the final term describes the energy exchange between the gas and solid phases. The diffusion coefficient is calculated using the following expression [15]:

$$\kappa_{\Theta_{s}} = \frac{15d_{s}\rho_{s}\alpha_{s}\sqrt{\Theta_{s}\pi}}{4(41-33\eta)} \left[1 + \frac{12}{5}\eta^{2}(4\eta - 3)\right. \\
\left. \cdot \alpha_{s}g_{0,ss} + \frac{16}{15\pi}(41-33\eta)\eta\alpha_{s}g_{0,ss}\right],$$
(13)

where η is a dimensionless parameter calculated as:

$$\eta = \frac{1}{2} \left(1 + e_{ss} \right). \tag{14}$$

The collisional dissipation of energy represents the rate at which energy is dissipated within the solid phase due to collisions between particles. It is calculated using the following equation [17]:

$$\gamma_{\Theta_{s}} = \frac{12(1 - e_{ss}^{2})g_{0,ss}}{d_{s}\sqrt{\pi}}\rho_{s}\alpha_{s}^{2}\Theta_{s}^{\frac{3}{2}}.$$
(15)

Lastly, the interphase energy transfer is described by the following equation [18]:

$$\varphi_{\sigma s} = -3\beta\Theta_{s}.\tag{16}$$

In this work, the Syamlal-O'Brien drag model, which is based on the terminal velocity of particles, is employed [19]. The momentum exchange coefficient β is calculated using the following equation:

$$\beta = \frac{3\alpha_s \alpha_g \rho_g}{4v_{r,s}^2 d_s} C_D \left(\frac{Re_s}{v_{r,s}} \right) |\mathbf{v_s} - \mathbf{v_g}|, \tag{17}$$

where $v_{r,s}$ is the terminal particle velocity, d_s is the particle diameter, C_D is the drag coefficient, and Re_s is the Reynolds number for the solid phase. The drag coefficient, originally derived by Dalla Valle [20], is calculated as follows:

$$C_D = \left(0.63 + \frac{4.8}{\sqrt{\frac{Re_s}{v_{r,s}}}}\right)^2.$$
 (18)

The terminal particle velocity for the solid phase is calculated using the following expression [21]:

$$v_{r,s} = 0.5A - 0.03Re_s + 0.5\sqrt{(0.06Re_s)^2 + 0.12Re_s(2B - A) + A^2}$$
,(19) with

$$A = \alpha_g^{4.14},\tag{20}$$

and

$$B = \begin{cases} 0.8\alpha_g^{1.28} & \text{for } \alpha_g \le 0.85\\ \alpha_\sigma^{2.65} & \text{for } \alpha_g \ge 0.85 \end{cases}$$
 (21)

2.2 Coupled CFD-DEM

In the coupled CFD-DEM approach, the hydrodynamic behavior of the gas within a gas-solid fluidized bed is modeled using CFD to solve the conservation equations. The particles in the system are modeled using the discrete element method (DEM), which governs their motion and interactions based on Newton's second law of motion [22]. In the CFD-DEM coupling, the solid volume fraction field is computed using a volumetric diffusion Lagrangian-Eulerian mapping, which smoothly distributes each particle's volume to the surrounding cells while conserving the total solid phase volume. For particle i with mass m_i , the following set of equations is solved:

$$m_i \frac{d\mathbf{v_i}}{dt} = \sum_{j=1}^n \mathbf{F_{ij}^c} + \mathbf{F_i^f} + \mathbf{F_i^g}, \tag{22}$$

$$I_{i}\frac{d\mathbf{\omega_{i}}}{dt} = \sum_{j=1}^{n_{i}} \mathbf{M_{ij}},$$
(23)

where $\mathbf{v_i}$ is the translational velocity of the particle, ω_i is the angular velocity, $\mathbf{F_{ij}^c}$ and $\mathbf{M_{ij}}$ are the contact force and torque resulting from particle interactions with other particles and walls, $\mathbf{F_i^f}$ is the force due to particle-fluid interactions, $\mathbf{F_i^g}$ is the gravitational force, and I_i is the moment of inertia. Particle-particle and particle-wall interactions are described using a soft-sphere model, where normal and tangential forces relative to the contact are modeled separately [23]. The normal contact force component is modeled using the Hysteretic linear spring model [24], as shown below:

$$\mathbf{F}_{ij}^{\mathbf{n},\mathbf{t}} = \begin{cases} \min\left(K_{i}s', \mathbf{F}_{ij}^{\mathbf{n},(\mathbf{t}-\Delta\mathbf{t})} + K_{u}\Delta s\right) & \text{if} \quad \Delta s \ge 0\\ \max\left(\mathbf{F}_{ij}^{\mathbf{n},(\mathbf{t}-\Delta\mathbf{t})} + K_{u}\Delta s, 0.001K_{i}s'\right) & \text{if} \quad \Delta s \le 0 \end{cases}$$
(24)

$$\Delta s = s^t - s^{t-\Delta t},\tag{25}$$

where $\mathbf{F}_{ij}^{\mathbf{n},\mathbf{t}}$ and $\mathbf{F}_{ij}^{\mathbf{n},(\mathbf{t}-\Delta t)}$ are the normal forces acting on particle i at the current and previous time steps, Δt is the time step size, s is the contact overlap, and K_l and K_u are the loading and unloading contact stiffnesses, determined by the particle properties as:

$$\frac{1}{K_{I}} = \begin{cases}
\frac{1}{K_{L,p_{1}}} + \frac{1}{K_{L,p_{2}}} & \text{for particle-particle contact} \\
\frac{1}{K_{L,p}} + \frac{1}{K_{L,w}} & \text{for particle-wall contacts}
\end{cases}$$
(26)

$$K_u = \frac{K_l}{e_w^2},\tag{27}$$

where subscripts 1 and 2 represent two contacting particles. The individual stiffnesses associated with a particle and a wall are calculated as:

$$K_{l,p} = E_p L, (28)$$

$$K_{l,w} = E_w L, \tag{29}$$

where E is the Young's modulus and L is the particle size. The tangential contact force is modeled using the linear spring Coulomb limit model. If the tangential force is assumed to be purely elastic, it can be calculated using the following equation:

$$\mathbf{F}_{ii,e}^{\tau,t} = \mathbf{F}_{ii}^{\tau,(t-\Delta t)} - K_{\tau} \Delta s_{\tau}, \tag{30}$$

where $\mathbf{F}_{ij}^{\tau,(t-\Delta t)}$ is the tangential contact force at the previous time step, K_{τ} is the tangential stiffness, and Δs_{τ} is the tangential overlap difference between two time steps. Since this model does not allow the tangential force to exceed Coulomb's limit, the complete expression is given as follows:

$$\mathbf{F}_{ij}^{\tau,t} = \min\left(\left|\mathbf{F}_{ij,e}^{\tau,t}\right|, \mu \mathbf{F}_{ij,e}^{n,t}\right) \frac{\mathbf{F}_{ij,e}^{\tau,t}}{\left|\mathbf{F}_{ij,e}^{\tau,t}\right|},\tag{31}$$

where μ is the friction coefficient. For a more detailed description of the model, the reader is encouraged to consult the literature by Walton and Braun [24] and Cundall and Strack [22].

The effect of fluid flow across the particle bed is modeled using a two-way coupled CFD-DEM approach. The force $\mathbf{F_i^f}$ consists of drag and pressure contributions, as shown below:

$$\mathbf{F}_{\mathbf{n}} = -V_{\mathbf{n}} \Delta p,\tag{32}$$

$$\mathbf{F}_{\mathbf{D}} = \frac{1}{2} \beta \rho_{\mathbf{g}} A_{\mathbf{p}} |\mathbf{v}_{\mathbf{g}} - \mathbf{v}_{\mathbf{s}, \mathbf{i}}| (\mathbf{v}_{\mathbf{g}} - \mathbf{v}_{\mathbf{s}, \mathbf{i}}), \tag{33}$$

where V_p is the particle volume, Δp is the local pressure gradient, A_p is the projected particle area in the direction of the flow, and $\mathbf{v_g} - \mathbf{v_{s,i}}$ is the relative velocity between particle i and the fluid. The Syamlal-O'Brien drag model was again used to calculate the momentum exchange coefficient, as described in the equations shown above. In both numerical models, the $k-\omega$ SST turbulence model was employed [25].

2.3 Model Validation

The validation of both the TFM-KTGF and coupled CFD-DEM models was performed using a benchmark single-spout fluidized bed case. The simulation results were compared with experimental data reported by Van Buijtenen et al. [26]. In that study, particle velocities

were measured using particle image velocimetry (PIV) and positron emission particle tracking (PEPT) systems at two different heights: 0.05 m and 0.10 m from the bottom, as indicated by the red dashed lines in Fig. 2.

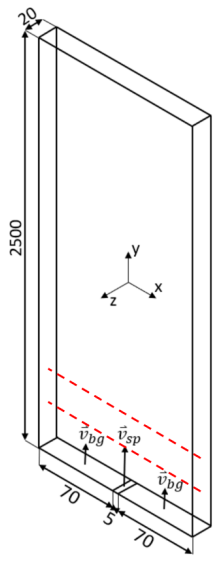


Fig. 2. Schematic of the single-spout fluidized bed used for model validation, where the red dashed lines indicate the locations where particle velocities were measured

Simulations were performed using two software packages: ANSYS Fluent [27] for hydrodynamics and ANSYS Rocky [28] for DEM. A uniform numerical mesh consisting of 58,000 hexahedral elements was used for both models. The system under study contained 12,000 spherical glass particles, each with a uniform diameter of 3 mm and a density of 2505 kg/m³. The restitution coefficients for all interactions were set to 0.97, while the friction coefficients for particle-particle and particle-wall interactions were set to 0.1 and 0.3, respectively, consistent with previous studies [26,29,30].

Table 1. Simulation parameters used for the validation study

Parameter	Value
Material	Glass
Number of particles, N	12000
Particle diameter, d_s	3 mm
Particle density, ρ_s	2505 kg/m ³
Restitution coefficient, e_{ss}	0.97
Particle-particle friction coefficient, μ_{p-P}	0.1
Particle-wall friction coefficient, μ_{p-w}	0.3
Spout velocity, $\mathbf{v_{sp}}$	43.5 m/s
Background velocity, $\mathbf{v_{bg}}$	2.4 s
Total simulation time, <i>t</i>	20 s
CFD time step, Δt_{CFD}	10 ⁻⁵ s

The spout and background velocities at the inlet were set to 43.5 m/s and 2.4 m/s, respectively, with the pressure outlet set to ambient pressure. All walls were assigned with no-slip boundary conditions. The total simulation time for both models was set to 20.0 s, with a CFD time step of 10^{-5} s, while the DEM time step was calculated automatically within ANSYS Rocky based on the hysteretic linear spring model [31]. A summary of all simulation parameters used in this study is presented in Table 1.

Figure 3 compares the particle velocity profiles in *y* direction at different simulation times. Figures 3a, b and c show results from the TFM-KTGF approach, while Figs. 3d, e and f present results from

the coupled CFD-DEM approach at t = 6 s (Figs. 3a and d), t = 18 s (Figs. 3b and e), and as a time-averaged profile (Figs. 3c and f).

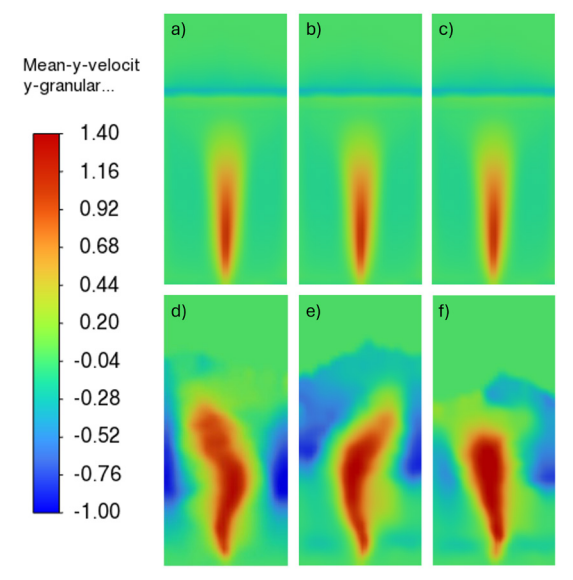


Fig. 3. a), b) and c) Average particle velocity in the y direction obtained using the TFM-KTGF approach, and d) e) and f) coupled CFD-DEM approach at:
a) and d) t = 6 s, b) and e) t = 18 s, and c) and f) as a time-averaged result

It is evident that the particle velocities obtained using the TFM-KTGF approach exhibit a very uniform profile throughout the simulation. This behavior arises from the nature of the TFM-KTGF model, in which particles are treated as a continuum phase. In this framework, there is no discrete mechanism driving the fluid to interact with particles in a way that would cause substantial variations in the velocity profile over time. In contrast, the velocity profiles obtained from the coupled CFD-DEM approach show a noticeable change as time progresses. This is because the direct interactions between particles and the airflow influence particle velocities, causing the profile to evolve dynamically over time.

The time-averaged particle velocity profiles in y direction, along the length of the fluidized bed at heights of 0.05 m and 0.10 m from the bottom, were compared with experimental data. The results are shown in Fig. 4. Good agreement between the numerical model predictions and the experimental data is observed, particularly at the height of 0.05 m from the bottom. Both numerical models produced similar velocity trends, demonstrating the validity of both approaches for simulating fluidized bed behavior.

Figure 5 shows the time-averaged particle velocity vectors obtained from PIV and PEPT measurements by Van Buijtenen et al. [26], along with the corresponding results from this study. Good agreement was observed between both the TFM-KTGF and coupled CFD-DEM approaches and the experimental data. In the coupled CFD-DEM approach, intensive circulation patterns are clearly visible, closely matching the experimental observations from PIV and PEPT. In contrast, the TFM-KTGF results show less pronounced circulation. The slight differences observed between the PIV and PEPT vector fields are attributed to challenges inherent in the experimental setup, as described by Van Buijtenen et al. [26].

In summary, both the TFM-KTGF and coupled CFD-DEM approaches for simulating single-spout fluidized beds provide satisfactory predictions of flow dynamics when compared with experimental results obtained using PIV and PEPT, despite slight deviations. Both models showed good agreement with the experimental particle velocity data, as shown in Fig. 3, confirming

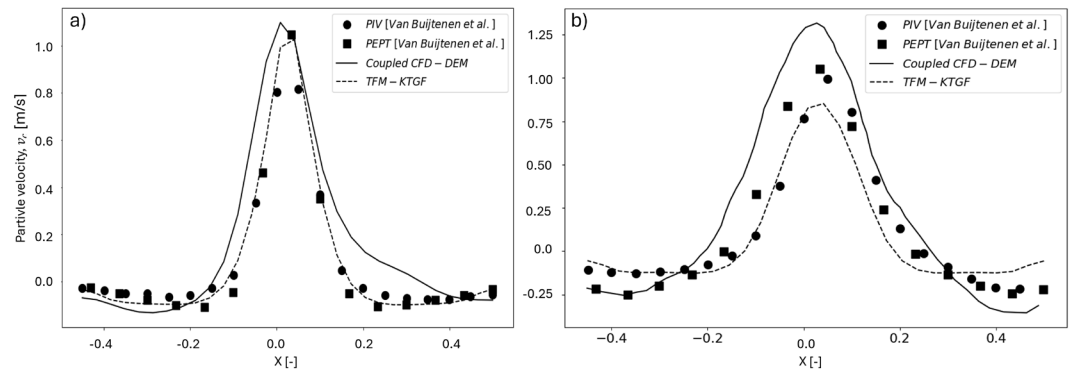


Fig. 4. Time-averaged particle velocity profiles in y direction along the length of the single-spout fluidized bed system at heights of a) 0.05 m, and b) 0.10 m from the bottom

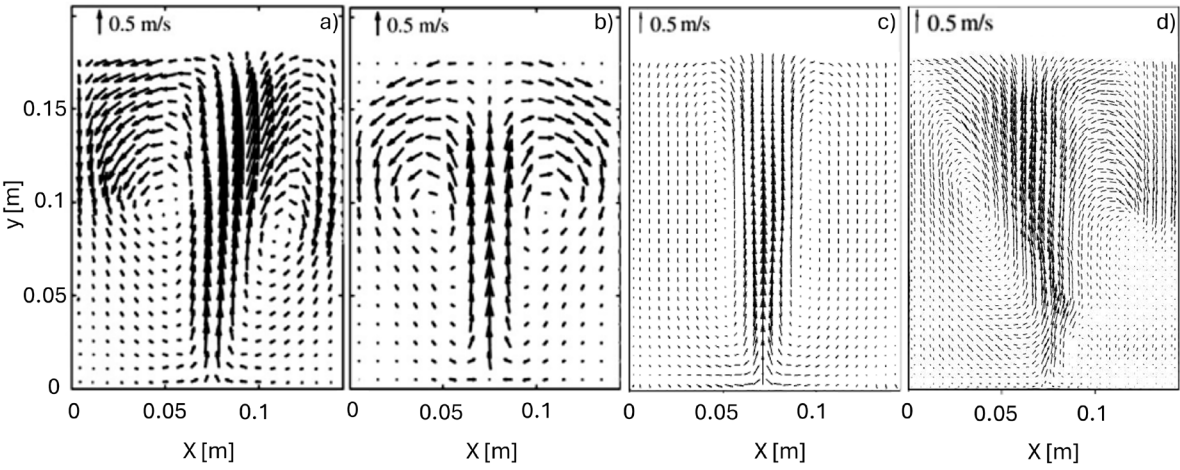


Fig. 5. Time-averaged particle velocity vector fields in the single-spout fluidized bed system; a) velocity PIV [26], b) velocity PEPT [26], velocity TFM-KTGF, and d) velocity coupled CFD-DEM

their reliability of these models for further analyses of flow distribution through a non-uniform distribution plate.

2.4 Flow Distribution Analysis

The flow distribution analysis was conducted on the geometry of a laboratory-scale fluidized bed system with a non-uniform distribution plate, as shown in Fig. 6. The colored sections on the distribution plate (Fig. 6c) represent different groups of openings: cyan indicates 4 mm, magenta 3.5 mm, red 3 mm, blue 1 mm, and green 2 mm. To reduce computational cost and simulation time, the geometry was symmetrically reduced to a quarter section, while preserving the essential flow characteristics.

As in the validation study, ANSYS Fluent [27] and ANSYS Rocky [28] were used to simulate multiphase flow using the TFM-KTGF and coupled CFD-DEM numerical models, respectively. Both approaches used the same numerical mesh, consisting of 1.5 million polyhedral elements. The simulations were performed with a total of 300 g of zeolite particles, with diameters ranging from 0.5 mm to 5 mm. The detailed particle size distribution is provided in Table 2, and the bulk particle density was set to 770 kg/m³. These values were selected based on the work of Zadravec et al. [32] to reflect realistic conditions in a laboratory-scale fluidized bed system. In the TFM-KTGF approach, where particles are represented as a continuous phase, the particle size distribution was first determined using the population balance model (PBM). The discrete method was applied, in which the overall particle size distribution is discretized into a finite number of size classes. From this distribution, the Sauter mean diameter was evaluated and used in the TFM-KTGF model. This ensures that the influence of the particle size distribution is captured in an averaged

manner while maintaining the computational framework of the two-fluid model. The interaction parameters, including restitution and friction coefficients for particle-particle and particle-wall contacts, were based on literature values [32] and are summarized in Table 3.

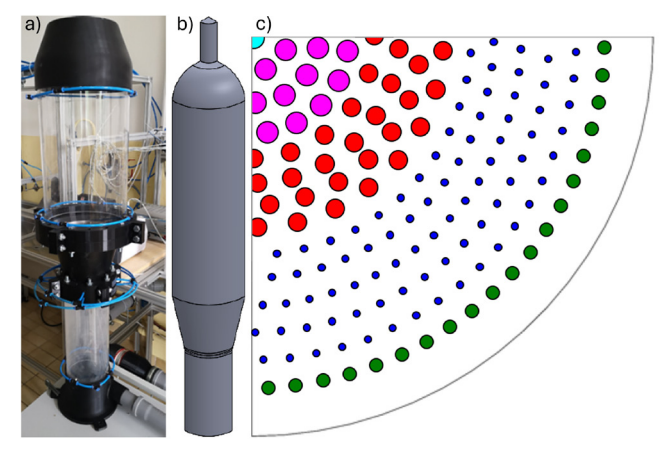


Fig. 6. a) Laboratory-scale fluidized bed system, b) the simplified geometry, and c) distribution plate geometry used in the analysis

Air was introduced into the system through the bottom inlet at volume flow rates ranging from 50 m³/h to 70 m³/h, increasing in increments of 5 m³/h to examine the effect of inlet velocity on flow distribution. Ambient pressure was applied at the outlet, and symmetry boundary conditions were imposed on the cut planes to represent the quarter geometry. All other walls were assigned no-slip boundary conditions to accurately capture near-wall interactions.

The total simulation time for each case was set to 5 s, with a CFD time step size of 10^{-4} s, while the DEM time step was calculated automatically, as in the validation case [31]. This ensured sufficient temporal resolution to capture flow evolution and particle behavior throughout the system.

Table 2. Zeolite particle size distribution

Particle size [mm]	0.5	1.0	2.0	3.15	5.0
Mass fraction [%]	0.5	0.8	3.5	77.3	17.9

Table 3. Restitution and friction coefficients used in this analysis

	Particle-Particle	Particle-Wall
Restitution coefficient	0.1	0.5
Friction coefficient	0.6	0.5

The complete set of parameters used in flow distribution simulations is summarized in Table 4.

Table 4. Simulation parameters used for the flow distribution study

Value		
Zeolite		
300 g		
Table 2		
770 kg/m ³		
Table 3		
Table 3		
[50, 55, 60, 65, 70] m ³ /h		
5.0 s		
10 ⁻⁴ s		

3 RESULTS AND DISCUSSION

To thoroughly examine the effect of particsles on airflow distribution through the fluidized bed distribution plate, multiple simulation cases were performed. These included simulations of the system without particles, to establish the baseline flow distribution in an empty geometry, and simulations with particles using the TFM-KTGF and coupled CFD-DEM models to assess the influence of particles on flow distribution.

The objective was to compare the simulation results with the theoretical flow distribution, which assumes that air distributes proportionally according to sthe opening fraction of each hole size group on the distribution plate. In other words, the flow rate through each group of openings was assumed to correspond to its relative area fraction on the plate.

Figure 7 compares the theoretical flow distribution, based on the open-area fraction, with the simulation results under different operating conditions. The solid lines represent the theoretical flow fractions for each group of openings, while the symbols and dashed lines correspond to the simulation data at various inlet flow rates. Results are presented for both an empty system (without particles) and a fluidized system (with particles), evaluated using two multiphase modeling approaches: TFM-KTGF and coupled CFD-DEM. The figure illustrates that the actual flow distribution deviates from the theoretical prediction even in the absence of particles, with these deviations becoming more pronounced when particles are introduced. In particular, the system containing particles shows clear shifts in the flow fractions through each opening group (e.g. 3 mm, 3.5 mm and 4 mm opening groups experience increased flow relative to the geometric assumption, while the 1 mm and 2 mm groups exhibit reduced flow). Furthermore, increasing the inlet air flow rate slightly

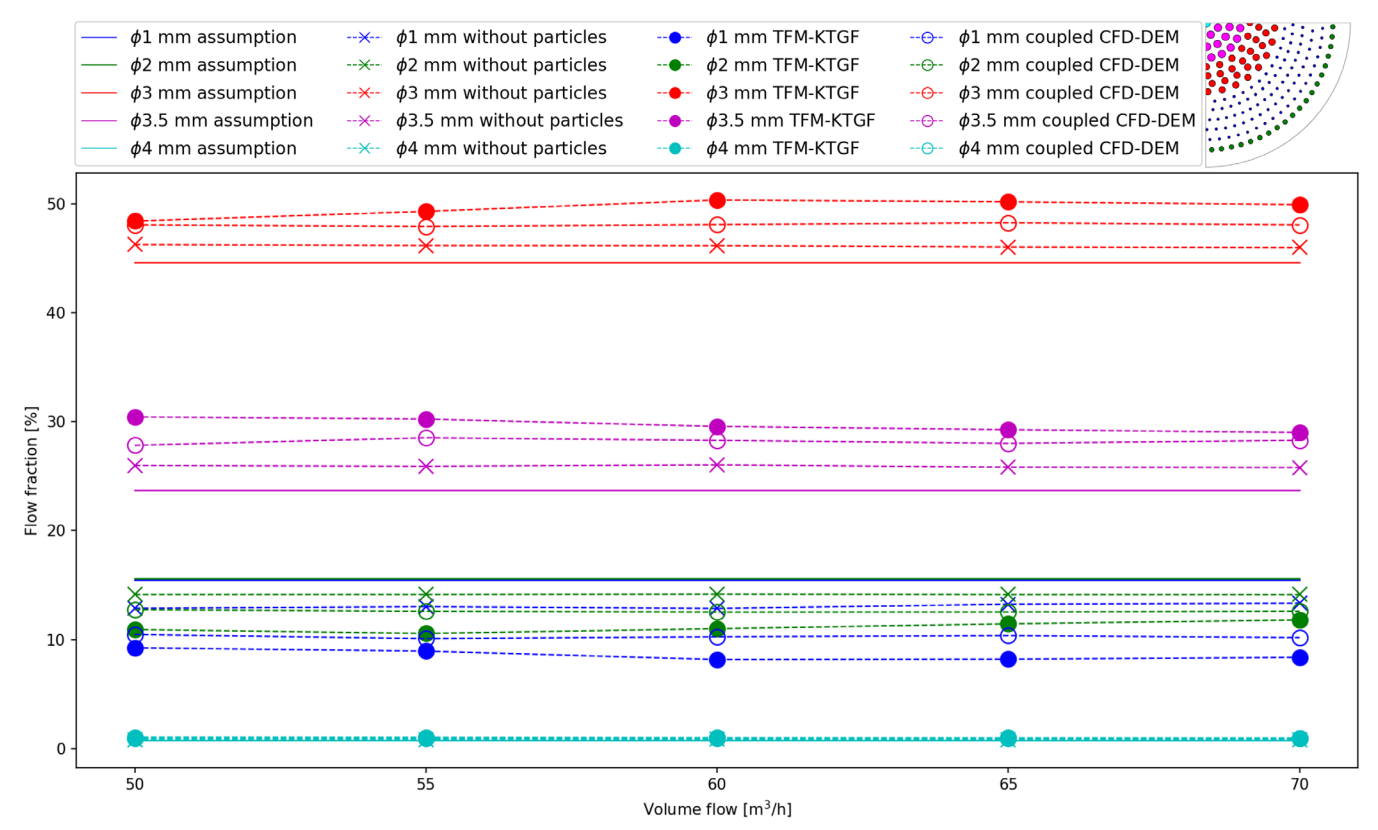


Fig. 7. Flow distribution through distribution plate openings of different sizes at various inlet air volume flow rates

alters the distribution, indicating that operating conditions influence how gas is channeled through the distributor.

These findings highlight that particle interactions introduce additional resistance and non-uniformity in local flow paths that cannot be captured by geometric assumptions alone, emphasizing the importance of modeling approaches that explicitly account for the particle phase.

A broader overview of the flow distribution is presented in Fig. 8, where the flow fractions for each opening size group are averaged across all inlet air flow rates. The results again confirm a significant mismatch between the theoretical distribution and the actual simulated distribution, particularly in the presence of particles.

Differences between the results obtained using the TFM-KTGF approach and those from the coupled CFD-DEM approach are also evident. These differences stem from the fundamental modeling approaches: TFM-KTGF treats the particle phase as a continuum, whereas the coupled CFD-DEM explicitly tracks individual particles. This distinction influences not only the flow predictions but also the computational performance of each model.

From a computational perspective, the TFM-KTGF approach proved to be significantly more efficient. Because it does not resolve individual particle trajectories, it requires far fewer computational resources than the coupled CFD-DEM model, which solves the equations of motion for each particle. In our simulations, the TFM-KTGF model completed each run approximately five times faster than the coupled CFD-DEM model on the same hardware. This substantial difference in computational time underscores the appeal of TFM-KTGF for large-scale simulations involving high particle counts.

4 CONCLUSIONS

In this study, we investigated gas flow distribution through a non-uniform distribution plate in a laboratory-scale fluidized bed system using two numerical approaches: TFM-KTGF and coupled CFD-DEM. Both approaches were employed to examine their behavior and predictive capability in a laboratory-scale fluidized bed. CFD-DEM provides detailed particle behavior, capturing particle-fluid interactions and heterogeneities, while TFM-KTGF efficiently predicts global flow trends. Using both methods allows us to evaluate how particle effects influence gas distribution and to assess the validity of the continuum assumptions in the TFM framework. Both models were validated against experimental data from a single-spout fluidized bed and demonstrated satisfactory agreement in predicting particle velocity profiles and overall flow behavior. These results confirm that both approaches can capture the essential features of fluidized bed dynamics.

This study demonstrates that particle effects can substantially alter the flow distribution in non-uniform distribution plates, despite the conventional assumption that gas flows proportionally to open area. By explicitly comparing the TFM-KTGF and coupled CFD-DEM approaches, we evaluated these deviations and provided evidence that particle-fluid interactions must be considered in distributor design. Incorporating the non-uniform plate geometry alongside realistic particle behavior bridges the gap between theoretical assumptions and actual flow patterns, offering a framework to guide improved design strategies for laboratory-scale fluidized beds.

Both numerical approaches captured the dynamic behavior of the particles, albeit with some differences.

The coupled CFD-DEM approach provided more detailed results by tracking individual particles, their interactions, and their influence on the flow, highlighting particle-fluid interactions that are not captured by simple geometric assumptions. In contrast, the

TFM-KTGF approach treats the particle phase as a continuum, which smooths out these details but still accurately represents the overall behavior on a global scale. A key advantage of the TFM-KTGF approach is its computational efficiency: in this study, it completed the simulations approximately five times faster than the coupled CFD-DEM approach on the same hardware, making it a practical choice for larger systems.

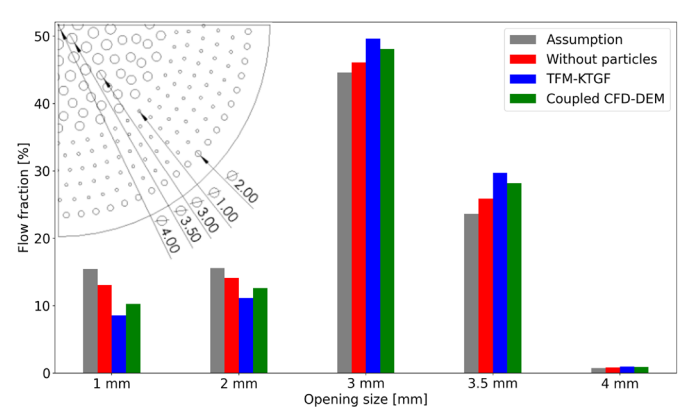


Fig. 8. Flow distribution through distribution plate openings of different sizes, averaged across all inlet air volume flow rate cases

While the coupled CFD-DEM approach captures particle-scale effects with high fidelity, its computational cost makes applications to large or industrial-scale fluidized beds impractical with current resources. Conversely, the TFM-KTGF model, though efficient, relies on a continuum treatment of the granular phase, which may smooth out local heterogeneities such as clustering or jet instabilities. These differences highlight that each model has inherent limitations, and their predictions should be interpreted within the context of laboratory-scale systems.

It should be emphasized that the present simulations were performed for laboratory-scale geometries, and direct extrapolation of the findings to full industrial-scale fluidized beds requires caution. Although the observed trends provide valuable guidance for distributor plate design, additional validation at pilot or industrial scale would be necessary to fully confirm the transferability of these results. Future work should therefore focus on bridging the gap between laboratory validation and industrial application.

References

- [1] Daizo, K., Levenspiel, O. *Fluidization Engineering*, 2nd ed. Butterworth Publishers, Stoneham (1991).
- [2] Fan, L.S., Zhu, C. Principles of Gas-Solid Flows. Cambridge University Press, Port Chester (1999) D0I:10.1017/CB09780511530142.
- [3] Michaelides, E.E., Sommerfeld, M., van Wachem, B. Multiphase Flows with Droplets and Particles, 3rd ed. CRC Press, Boca Raton (2022) D0I:10.1201/9781003089278.
- [4] Esgandari, B., Rauchenzauner, S., Goniva, C., Kieckhefen, P., Schneiderbauer, S. A comprehensive comparison of two-fluid model, discrete element method and experiments for the simulation of single- and multiple-spout fluidized beds. *Chem Eng Sci* 267 118357 (2023) D0I:10.1016/j.ces.2022.118357.
- [5] Ostermeier, P., Vandersickel, A., Gleis, S., Spliethoff, H. Numerical approaches for modeling gas-solid fluidized bed reactors: Comparison of models and application to different technical problems. J Energy Resour Technol 141 070707 (2019) D0I:10.1115/1.4043327.
- [6] Liu, D., van Wachem, B. Comprehensive assessment of the accuracy of CFD-DEM simulations of bubbling fluidized beds. *Powder Technol* 343 145-158 (2019) D0I:10.1016/j.powtec.2018.11.025.
- [7] Agrawal, V., Shinde, Y., Shah, M.T., Utikar, R.P., Pareek, V.K., Joshi, J.B. Effect of drag models on CFD-DEM predictions of bubbling fluidized beds with Geldart D particles. Adv Powder Technol 29 2658-2669 (2018) D0I:10.1016/j. apt.2018.07.014.

- [8] Zhang, Q., Cai, W., Lu, C., Gidaspow, D., Lu, H. Modified MFIX code to simulate hydrodynamics of gas-solids bubbling fluidized beds: A model of coupled kinetic theory of granular flow and discrete element method. *Powder Technol* 357 417-427 (2019) D0I:10.1016/j.powtec.2019.08.056.
- [9] Alobaid, F., Epple, B. Improvement, validation and application of CFD/DEM model to dense gas-solid flow in a fluidized bed. *Particuology* 11 514-526 (2013) D0I:10.1016/j.partic.2012.05.008.
- [10] Geldart, D., Baeyens, J. The design of distributors for gas-fluidized beds. Powder Technol 42 (1985) 67-78, D0I:10.1016/0032-5910(85)80039-5.
- [11] Karri, S.B.R., Knowlton, T.M. 4 Gas distributor and plenum design in fluidized beds. Yang, W.-C. (ed.) Fluidization, Solids Handling, and Processing, William Andrew Publishing, Westwood 209-235 (1999) D0I:10.1016/B978-081551427-5.50006-5.
- [12] Kevorkijan, L., Zadravec, M. Numerične simulacije toka tekočine in delcev v granulatorju z lebdečim slojem. Anali PAZU 12 17-30 (2022) D0I:10.18690/ analipazu.12.1.17-30.2022.
- [13] Gonzalez-Arango, D.I., Herrera, B. Evaluation of the flow distribution system influence on mixing efficiency in a fluidized bed for low-size Geldart B particles: A case study using CFD. S Afr J Chem Eng 52 325-335 (2025) D0I:10.1016/j. saice.2025.03.007.
- [14] Singh, R., Marchant, P., Golczynski, S. Modeling and optimizing gas solid distribution in fluidized beds. *Powder Technol* 446 120145 (2024) DOI:10.1016/j. powtec.2024.120145.
- [15] Syamlal, M., Rogers, W., O'Brien, T. MFIX Documentation: Theory Guide US Department of Energy, Morgantown (1993) D0I:10.2172/10145548.
- [16] Gidaspow, D., Bezburuah, R., Ding, J. Hydrodynamics of circulating fluidized beds, kinetic theory approach. 7th Fluidization Conference 75-82 (1992).
- [17] Lun, C., Savage, S., Jeffrey, D., Chepurniy, N. Kinetic theories for granular flow: Inelastic particles in Couette flow and slightly inelastic particles in a general flowfield. J Fluid Mech 140 223-256 (1984) DOI:10.1017/S0022112084000586.
- [18] Ding, J., Gidaspow, D. A bubbling fluidization model using kinetic theory of granular flow, *AIChE J* 36 523-538 (1990) **D0I:10.1002/aic.690360404**.
- [19] Syamlal, M., O'Brien, T. A Generalized Drag Correlation for Multiparticle Systems, Unpublished report (1987).
- [20] Dalla Valle, J.M. Micrometrics, the Technology of Fine Particles, Pitman (1948).
- [21] Garside, J., Al-Dibouni, M.R. Velocity-voidage relationships for fluidization and sedimentation in solid-liquid systems. *Ind Eng Chem Process Des Dev* 16 206-214 (1977) D0I:10.1021/i260062a008.
- [22] Cundall, P.A., Strack, O.D.L. A discrete numerical model for granular assemblies. Géotechnique 29 (1979) 47-95 D0I:10.1680/geot.1979.29.1.47.
- [23] Wassgren, C., Curtis, J.S. The application of computational modeling to pharmaceutical materials science. MRS Bull 31 900-904 (2006) D0I:10.1557/ mrs2006.210.
- [24] Walton, O.R., Braun, R.L. Viscosity, granular-temperature, and stress calculations for shearing assemblies of inelastic, frictional disks. *Journal Rheol* 30 949-980 (1986) D0I:10.1122/1.549893.
- [25] Menter, F.R. Two-equation eddy-viscosity turbulence models for engineering applications. AIAA Journal 32 1598 (1994) D0I:10.2514/3.12149.
- [26] van Buijtenen, M.S., van Dijk, W.J., Deen, N.G., Kuipers, J.A.M., Leadbeater, T., Parker, D.J. Numerical and experimental study on multiple-spout fluidized beds. Chem Eng Sci 66 (2011) 2368-2376 D0I:10.1016/j.ces.2011.02.055.
- [27] ANSIS Inc. Ansys® Academic Research, Release 23.1, Help System, Solver Theory, Multiphase Flow Theory, ANSIS (2023).
- [28] ANSIS Inc. Ansys® Academic Research, Release 23.1, Help System, DEM-CFD Coupling Technical Manual, ANSIS (2023).
- [29] Jajcevic, D., Siegmann, E., Radeke, C., Khinast, J.G. Large-scale CFD-DEM simulations of fluidized granular systems. Chem Eng Sci 98 298-310 (2013) D0I:10.1016/j.ces.2013.05.014.

- [30] Goniva, C., Kloss, C., Deen, N.G., Kuipers, J.A., Pirker, S. Influence of rolling friction on single spout fluidized bed simulation. *Particuology* 10 582-591 (2012) D0I:10.1016/j.partic.2012.05.002.
- [31] ANSIS Inc. Ansys® Academic Research, Release 25.1, Rocky Technical Manual: 5.2. Timestep Calculation, ANSIS (2023).
- [32] Zadravec, M., Orešnik, B., Hriberšek, M., Marn, J. Two-step validation process of particle mixing in a centrifugal mixer with vertical axis. *Proc Inst Mech Eng-E* 232 29-37 (2018) D0I:10.1177/0954408916678267.

Acknowledgements The authors would like to express their sincere gratitude to the professors, assistants, and colleagues at the Faculty of Mechanical Engineering, University of Maribor for their valuable support and constructive discussions throughout this work. We also gratefully acknowledge the financial support provided by the Slovenian Research Agency (ARRS) under the framework of Research Program P2-0196: Power, Process, and Environmental Engineering.

Received: 2025-04-23, Revised: 2025-09-09, Accepted: 2025-09-24 as Original Scientific Paper 1.01.

Data availability The data that support the findings of this study are available from the corresponding author upon reasonable request.

Authors contribution Matija Založnik: Formal analysis, Investigation, Writting - original draft, Writing - review & editing, Software, Visualization; Matej Zadravec: Methodology, Project Administration, Supervision.

Analiza distribucije toka plina v lebdečem sloju z uporabo modela dveh tekočin s kinetično teorijo granularnega toka in sklopljenega CFD-DEM: numerična študija

Povzetek Sistemi z lebdečim slojem se pogosto uporabljajo v kemičnem in procesnem inženirstvu zaradi svojih odličnih sposobnosti prenosa toplote in snovi. Numerično modeliranje ima ključno vlogo pri razumevanju in optimizaciji teh sistemov, pri čemer se med vodilne uveljavljata model dveh tekočin, dopolnjen s kinetično teorijo granularnega toka (TFM-KTGF) in sklopljena računalniške dinamike tekočin z metodo diskretnih elementov (CFD-DEM). V tej študiji sta uporabljena oba modela za simulacijo interakcij med plinom in trdnimi delci ter ovrednotena njuna učinkovitost na primeru eksperimentalnega primera iz literature. Analiziran je bil tudi vpliv delcev na porazdelitev toka plina skozi ne-uniformno distribucijsko ploščo. Rezultati kažejo, da je pogosta predpostavka o sorazmerni porazdelitvi toka glede na delež odprtin nepravilna, zlasti v prisotnosti delcev. Oba numerična modela zajameta to vedenje, pri čemer TFM-KTGF kaže trende primerljive s sklopljenim CFD-DEM pristopom a pri bistveno nižjih računskih časih. Ugotovitve poudarjajo pomen upoštevanja dinamike delcev pri oblikovanju distribucijskih plošč ter promovirajo uporabo TFM-KTGF kot obetavno alternativo za simulacije na velikih sistemih.

Ključne besede lebdeči sloj, distribucijska plošča, model dveh tekočin s kinetično teorijo granularnega toka, sklopljen CFD-DEM, distribucija toka